Interfacial Tension at the Boundary Between Nematic and Isotropic Phases of a Hard Rod Solution

Donald L. Koch*

School of Chemical Engineering, Cornell University, Ithaca, New York 14853

Oliver G. Harlen

Department of Applied Mathematical Studies, University of Leeds, Leeds LS2 9JT, U.K.

Received May 15, 1998; Revised Manuscript Received October 26, 1998

ABSTRACT: The excess surface free energy per unit area or interfacial tension is determined for hard-rod isotropic and nematic phases coexisting at equilibrium. The number density and order parameter profiles across the interface are obtained by minimizing the free energy in the inhomogeneous fluid using an approach that generalizes Onsager's classical theory to spatially inhomogeneous hard rod solutions. The excess surface free energy is a minimum when the director in the bulk of the nematic phase is at a 90° angle to the surface normal, indicating that this tangent alignment is the preferred orientation likely to be observed in practice. The surface tension for a tangent director is found to be $0.316k_BT/(dL)$, where k_B is Boltzmann's constant, T the absolute temperature and d and L are the diameter and length of the rods. The dependence of the rod concentration on position across the interface is nonmonotonic.

1. Introduction

A solution of hard rods with a large ratio of rod length L to diameter d is the simplest physical system that exhibits a phase transition from an isotropic to a nematic liquid crystalline phase. Consequently, this system is widely studied to obtain a qualitative guide to the thermodynamic and rheological properties of liquid crystal polymers. More quantitative comparisons with the hard rod theory may be undertaken for a few special physical systems such as tobacco mosaic virus and PBLG.[1−3] Over a certain range of total rod concentrations, the nematic phase coexists with an isotropic phase. The purpose of the present investigation is to determine the molecular structure of the interface between nematic and isotropic regions and the excess surface free energy or interfacial tension.

One motivation for studying this problem is the intrinsic interest in completing the characterization of the thermodynamics of the isotropic−nematic transition initiated by Onsager.[4] However, the study is also of interest as a simple prototype for spatially inhomogeneous liquid crystals. It will be seen that the number density and orientation distribution vary across the isotropic-nematic interfacial region over a thickness comparable with the rod length L. In a similar manner, the director (or direction of mean local molecular orientation) varies over a molecular length scale in the core of a defect of the type that are ubiquitous in sheared liquid crystalline polymers. The planar geometry of the isotropic−nematic interphase boundary makes this the simplest example of a spatially nonuniform hard rod system. The theoretical treatment of this problem may provide a useful background for future attempts to describe the energy of defect cores.

Onsager[4] showed that the transition from an isotropic to a nematic hard rod phase results from a competition between the decreased orientational entropy and increased translational entropy arising in the presence of orientational order. For rods of length L and diameter d, this transition occurs at number densities of order $1/(L^2d)$. He showed that, for high aspect ratio rods, $L/d \gg 1$, the changes in translational entropy are dominated by two-body excluded volume and the higher order terms in a virial expansion may be neglected at the concentration of the phase transition. The requirement of minimum free energy in the nematic phase leads to an integral equation for the distribution of rod orientations relative to the director. Solving this equation simultaneously with the requirements of equal osmotic pressure and chemical potential in the isotropic and nematic phases yields a solution for the number densities of the two coexisting phases and the orientation distribution of the nematic phase. To simplify the calculation, Onsager used a one parameter trial function

$$f = \frac{\alpha \cosh(\alpha \cos\theta)}{4\pi \sinh \alpha} \tag{1}$$

for the orientation distribution in the nematic phase. Here, α is a constant, θ is the angle of the rod's axis relative to the director, and f is the probability density function for the rods' orientation. This orientation distribution is normalized such that

$$\int d\mathbf{p}\, f = 1 \tag{2}$$

where $\mathbf{p}$ is a unit vector parallel to the axis of a rod and the domain of integration is the unit sphere. The degree of alignment in the nematic phase is usually characterized in terms of the order parameter

$$\langle P_2 \rangle = \int d\mathbf{p}\, f \left(\frac{3}{2}\cos^2\theta - \frac{1}{2}\right) \tag{3}$$

which is equal to zero in the isotropic phase and one if the rods are all aligned parallel to the director. Using Onsager's trial function, the order parameter may be related simply to α as

$$\langle P_2 \rangle = 1 + \frac{3}{\alpha^2} - \frac{2}{\alpha}\coth\alpha \tag{4}$$

10.1021/ma980779l CCC: $18.00
Published on Web 12/22/1998

Onsager found the order parameter at coexistence to be $\langle P_2 \rangle = 0.847$ and the number densities of the isotropic and nematic phases to be $n_I = 4.25/(L^2 d)$ and $n_N = 5.71/(L^2 d)$, respectively.

A more precise calculation of the number densities and order parameter at the phase transition can be achieved if the simple trial function, (3), for the rod orientation distribution is replaced by a general expansion in terms of Legendre polynomials. Using this approach, Lekkerkerker *et al.*[5] showed that the coexistence conditions are $\langle P_2 \rangle = 0.792$, $n_I = 4.19/(L^2 d)$, and $n_N = 5.33/(L^2 d)$.

Bolthuis and Frenkel[13] performed Monte Carlo simulations to study the isotropic−nematic transition in a system of hard spherocylinders over a wide range of aspect ratios. This study confirmed the validity of the analytical theory[5] in the limit of high aspect ratio $L/d \gg 1$. However, a quite large aspect ratio $L/d = 50$ is required before the transition number density n_I is within 10% of its asymptotic value. While the analytical theory for high-aspect-ratio hard rigid rods yields the correct physics, the detailed behavior of experimentally accessible systems is likely to be affected by finite aspect ratio, polymer flexibility, and electrostatic or other interactions.

The contribution of variations in the director that occur over length scales large compared with the molecular length to the free energy of a liquid crystal may be treated using Frank elasticity theory.[6] Straley[7] has computed the Frank elastic constants for a hard rod solution.

Doi and Kuzuu[8] derived a theoretical estimate of the surface tension at the boundary between isotropic and nematic phases of a hard rod solution using an approach that treated the interfacial thickness as a macroscopic length scale. They used the Onsager trial function, (1), and assumed that α and the number density of rods, n, varied with the spatial coordinate z according to

$$\alpha = \frac{\alpha_N}{2}\left[\tanh\left(\frac{z}{\delta}\right) + 1\right] \tag{5}$$

$$n = \frac{n_N - n_I}{2}\tanh\left(\frac{z}{\delta}\right) + \frac{n_N + n_I}{2} \tag{6}$$

where δ is the interfacial thickness and α_N is the value of α in the bulk nematic phase. Doi and Kuzuu expanded the free energy of the solution in terms of gradients of probability density and truncated this expansion at the level of first derivatives. The neglected higher order derivatives would be expected to make a small contribution if the interface were very thick, i.e., $\delta \gg L$. However, Doi and Kuzuu found that $\delta = 0.636L$ when the director is parallel to the interface. Thus, the interfacial thickness is of molecular size, and the truncated gradient expansion is inconsistent.

When the interfacial thickness is comparable with the molecular dimensions, a fully nonlocal description of the excluded volume rod−rod interactions is required. In this paper, such a description will be developed by generalizing Onsager's analysis to a probability density function for the rods that varies in positional as well as orientational space. Thus, the minimization of the free energy gives rise to an equation involving integrals over z as well as $\mathbf{p}$. Our calculations will use either the Onsager trial function, (1), or a biaxial generalization of this function. However, no assumption will be made concerning the shape of the spatial profiles of number density and order parameter. The alternative to using an Onsager-like trial function is to expand the probability in a full spherical harmonic expansion.[11,12] However, this approach is more computationally expensive making it difficult to achieve an adequate spatial resolution. Like Doi and Kuzuu,[8] we will consider situations where the director is oriented at an angle θ_n relative to the unit normal to the interface. The value of θ_n that minimizes the surface free energy will be the thermodynamically preferred orientation that is expected to be observed experimentally.

2. Analysis

The contribution of the hard rods to the free energy of a spatially inhomogeneous solution, F, may be written as

$$\frac{F}{k_B T} = N \ln(n_I \Lambda^3) + \int d\mathbf{r}_1 \, \tilde{F} \tag{7}$$

where

$$\tilde{F} = \int d\mathbf{p}_1 \, P(\mathbf{r}_1, \mathbf{p}_1) \ln\left[\frac{4\pi P(\mathbf{r}_1, \mathbf{p}_1)}{n_I}\right] + \frac{1}{2}\int d\mathbf{p}_1 \, d\mathbf{p}_2 \, d\mathbf{r} \, P(\mathbf{r}_1, \mathbf{p}_1) P(\mathbf{r}_2, \mathbf{p}_2) B(\mathbf{r}, \mathbf{p}_1, \mathbf{p}_2) \tag{8}$$

Here, $\Lambda = h/(2\pi m k_B T)$ is the thermal de Broglie wavelength, h is Planck's constant, and m is the rod mass. The reference chemical potential is chosen to be unity when the probability density P is isotropic and spatially homogeneous with $P = 1/(4\pi\Lambda^3)$. The first term on the right-hand side of (8) represents the entropy associated with a solution of rods with a probability density P when the rods are allowed to overlap. The final term accounts for the decrease in entropy due to the excluded volume of pairs of rods. The interaction function $B(\mathbf{r}, \mathbf{p}_1, \mathbf{p}_2)$ has value one if two rods with orientation $\mathbf{p}_1$ and $\mathbf{p}_2$ and separation vector $\mathbf{r} = \mathbf{r}_2 - \mathbf{r}_1$ overlap and is zero otherwise. This expression for the free energy reduces to that forming the basis of Onsager's analysis when P is independent of spatial position.

In writing (8), we have neglected the excluded volumes involving three or more rods. The neglected, three-body term is of order $Nn^2L^3d^3$ whereas the two-body term is of order NnL^2d. The three-body term is order d/L smaller than the two-body term at the number densities (order $1/(L^2 d)$) at which the isotropic−nematic phase coexistence occurs. For high aspect ratio fibers, the overlap function B may be approximated by

$$B(\mathbf{r}, \mathbf{p}_1, \mathbf{p}_2) = 2d \, \delta\left[\mathbf{r}\cdot\frac{\mathbf{p}_1 \times \mathbf{p}_2}{|\mathbf{p}_1 \times \mathbf{p}_2|}\right] \Pi(\mathbf{r}\cdot\mathbf{p}_1/L)\Pi(\mathbf{r}\cdot\mathbf{p}_2/L) \tag{9}$$

where

$$\Pi(x) = \begin{cases} 1 & \text{if } |x| < \frac{1}{2} \\ 0 & \text{if } |x| > \frac{1}{2} \end{cases} \tag{10}$$

and δ is the Dirac delta function. In writing (9), we have taken advantage of the fact that P varies only over the length scale L, so that we can neglect the small variation

in the probability density P when a rod center translates over a distance comparable with the rod thickness d.

We will consider an interface that is planar on the molecular length scale. The spatial coordinate z is chosen to be perpendicular to the plane of the interface. Equation 7 is applied to a right cylinder whose base A is parallel to the plane of the interface. The volume V of this cylinder and the area A are large, i.e., $V \gg L^3$ and $A \gg L^2$. The number N of rods in the volume is specified to be intermediate between $n_I V$ and $n_N V$, so that the volume will straddle the interface. We will define the plane $z = 0$ such that

$$\int d\mathbf{r}_1 \, (n(\mathbf{r}_1) - n_0) = 0 \tag{11}$$

where

$$n_0 = \begin{cases} n_N & z_1 > 0 \\ n_I & z_I < 0 \end{cases} \tag{12}$$

and $n = \int d\mathbf{p}_1 P$. The constraint in (11) implies that the control volume extends from $z = -H_I$ to $z = H_N$ where $H_I = (n_N V - N)/[A(n_N - n_I)]$ and $H_N = (N - n_I V)/[A(n_N - n_I)]$. It is also interesting to define a characteristic width ζ of the interface as

$$\zeta = \frac{2 \int d\mathbf{r}_1 \, |n_0 - n|}{n_N - n_I} \tag{13}$$

The free energy per unit volume (normalized by $k_B T$) may be expressed as the sum

$$\tilde{F} = \tilde{F}_0 + \tilde{F}' \tag{14}$$

of the free energy that would occur if the bulk phases did not interact, *i.e.*

$$\tilde{F}_0 = \tilde{F}_I + (\tilde{F}_N - \tilde{F}_I) H(z_1) \tag{15}$$

and an extra free energy $\tilde{F}'$ due to the interaction. The bulk free energies obtained from Onsager's analysis are $\tilde{F}_I = 14.2/(L^2 d)$ and $\tilde{F}_N = 25.4/(L^2 d)$. Substituting (14) and (15) into (7), the free energy of the control volume is

$$\frac{F}{k_B T} = N \ln(n_I \Lambda^3) + \frac{(n_N V - N)\, \tilde{F}_I + (N - n_I V)\, \tilde{F}_N}{n_N - n_I} + A \int_{-\infty}^{\infty} \tilde{F}' \, dz_1 \tag{16}$$

Here, we have extended the integration in the final term to $\pm\infty$ because the contributions from large values of $|z_1|$ are very small. Since the first two terms on the right-hand side of (16) are independent of interfacial area, the surface tension is simply

$$\gamma = \left(\frac{\partial F}{\partial A}\right)_{T,N,V} = k_B T \int_{-\infty}^{\infty} \bar{F}' \, dz_1 \tag{17}$$

To determine the rods' probability density, we must minimize the free energy with respect to variations in P subject to the constraint in (11) that the total number of rods in the control volume is fixed. As in Onsager's analysis, this will be accomplished by using a Lagrange multiplier λ so that the function to be minimized is

$$\int d\mathbf{r}_1 \, d\mathbf{p}_1 \, P(\mathbf{r}_1, \mathbf{p}_1) \ln\left[\frac{4\pi P(\mathbf{r}_1, \mathbf{p}_1)}{n_I}\right] + \frac{1}{2} \int d\mathbf{r}_1 \, d\mathbf{p}_1 \, d\mathbf{p}_2 \, d\mathbf{r} \, P(\mathbf{r}_1, \mathbf{p}_1) \, P(\mathbf{r}_2 = \mathbf{r} + \mathbf{r}_1, \mathbf{p}_2) \times B(\mathbf{r}, \mathbf{p}_1, \mathbf{p}_2) - \lambda \int d\mathbf{r}_1 \, d\mathbf{p}_1 \left[P(\mathbf{r}_1, \mathbf{p}_1) - \frac{n_0(\mathbf{r}_1)}{4\pi}\right]$$

and the minimization occurs when

$$\ln\left[\frac{4\pi P}{n_I}\right] + 1 - \lambda + \int d\mathbf{r} \, d\mathbf{p}_2 \, P(\mathbf{r}_2, \mathbf{p}_2) \, B(\mathbf{r}, \mathbf{p}_1, \mathbf{p}_2) = 0 \tag{18}$$

The value of the Lagrange multiplier may be determined as $\lambda = 7.68$ so that the number density takes on the value $n_I = 4.25/(L^2 d)$ determined by Onsager for the isotropic phase coexisting with a nematic phase.

Thus, if we nondimensionalize lengths by L and the probability density by $1/(L^2 d)$, the nondimensionalized probability density function $P(\mathbf{r}, \mathbf{p})$ satisfies the implicit equation

$$P(\mathbf{r}_1, \mathbf{p}_1) = 269.5 \exp(-J) \tag{19}$$

where

$$J = \int d\mathbf{r} \, d\mathbf{p}_2 \, P(\mathbf{r}_2, \mathbf{p}_2) \, B(\mathbf{r}, \mathbf{p}_1, \mathbf{p}_2) \tag{20}$$

and

$$B(\mathbf{r}, \mathbf{p}_1, \mathbf{p}_2) = 2 \, \delta\left[\mathbf{r} \cdot \frac{\mathbf{p}_1 \times \mathbf{p}_2}{|\mathbf{p}_1 \times \mathbf{p}_2|}\right] \Pi(\mathbf{r} \cdot \mathbf{p}_1) \, \Pi(\mathbf{r} \cdot \mathbf{p}_2)$$

The solution to the implicit equation, (19), for the probability density is computed using an iterative method, in which the multidimensional integral for J must be performed at each iteration.

Since the only spatial dependence of the probability density function is with respect to z, the integration in the plane perpendicular to the interface may be performed analytically to yield

$$J = 2 \int d\mathbf{p}_2 \int_{-a}^{a} dz_2 \, P(z_2, \mathbf{p}_2) |\mathbf{p}_1 \times \mathbf{p}_2| \, b(z_2) \tag{21}$$

where

$$a = \frac{1}{2}(\mu_1 + \mu_2) \tag{22}$$

$\mu_i = \mathbf{e}_z \cdot \mathbf{p}_i$, and $\mathbf{e}_z$ is a unit vector perpendicular to the interface. Here, $b(z)$ is a trapezoidal shaped function found from integrating the overlap function, and is given by

$$b = \begin{cases} (z + a)/(\mu_1 \mu_2) & \text{for } g > z > -a \\ (g - a)/(\mu_1 \mu_2) & \text{for } h > z > g \\ (a - z)/(\mu_1 \mu_2) & \text{for } a > z > h \end{cases} \tag{23}$$

where

$$g = \min\left[\frac{1}{2}(\mu_1 - \mu_2), \frac{1}{2}(\mu_2 - \mu_1)\right] \tag{24}$$

and

$$h = \max\left[\frac{1}{2}(\mu_1 - \mu_2), \frac{1}{2}(\mu_2 - \mu_1)\right] \quad (25)$$

provided μ_1 is nonzero. When μ_1 is zero, $b(z)$ is given by

$$b = \frac{1}{\mu_2} \quad (26)$$

After the probability distribution has been determined, the free energy per unit volume can be obtained from (8) and the surface tension from (17). The free energy scales with the thermal energy k_BT times the probability distribution, which is $O(1/L^2d)$ under two-phase coexistence conditions. Since the surface tension involves an integral of the $O(k_BT/L^2d)$ deviation of the free energy per unit volume from its bulk value across the $O(L)$ interface thickness, γ is proportional to k_BT/Ld.

3. Computational Issues

The probability density may be expressed as a product of the number density and an orientation distribution, so that

$$P(z_1, \mathbf{p}_1) = n(z_1)f(z_1, \mathbf{p}_1) \quad (27)$$

where f is normalized according to (2). In the first set of calculations presented below, we adopt the Onsager trial function, (1), allowing α to be a function of z_1

$$f(z_1, \mathbf{p}) = \frac{\alpha(z_1)}{4\pi \sinh \alpha(z_1)} \cosh[\alpha(z_1) \cos \theta] \quad (28)$$

where θ is the angle between the rod axis and the director. The director is taken to be at a fixed angle θ_n with respect to the normal to the interface. The director is not a function of z_1 as any change in θ_n would lead to a net torque on the interface. Later we will introduce a biaxial trial function that removes the constraint of axisymmetry about the director.

The spatial coordinate z_1 is discretized in intervals of Δz in the range $z_1 = (-H_\infty, H_\infty)$. For $z_1 > H_\infty$ and $z_1 < -H_\infty$, it is assumed that n and α take on their values in the bulk nematic and isotropic phase, respectively. Most of the computations were performed with $\Delta z = 0.02$ and $H_\infty = 1.6$. Halving Δz and doubling H_∞ were found to lead respectively to 1% and 0.05% changes in the surface tension for $\theta_n = 90°$. The three-dimensional integral in (21) was performed by numerical quadrature with the values of $\alpha(z_1)$ and $n(z_1)$ obtained by linear interpolation between the grid points.

Upon determining $\alpha(z_1)$ and $n(z_1)$, the surface tension was obtained from eqs 17 and 8. The integral over $\mathbf{r}$ in (8) can be simplified in a manner analogous to that used to obtain (21), so that the determination of the surface tension requires a six-dimensional integral involving the integration variables z_1, z_2, $\mathbf{p}_1$, and $\mathbf{p}_2$. The estimated error in the surface tension due to the numerical integration is 1−2%.

In principle, eq 19 should hold at all angles. However, since we are using an Onsager trial function, we require two equations for each grid point to determine the spatial profiles of n and α. For most of the calculations, we imposed the conditions that (19) be satisfied at $\theta = 13.9°$, *i.e.*

$$P(z_1, 13.9°) = 269.5 \exp[-J(z_1, 13.9°)] \quad (29)$$

and that the ratios of the probability densities at $\theta = 0°$ and $\theta = 37.8°$ be consistent with (19), i.e.

$$\frac{P(z_1, 0°)}{P(z_1, 37.8°)} = \exp[J(z_1, 37.8°) - J(z_1, 0°)] \quad (30)$$

The former condition may be thought of as an equation for the number density and the latter as an equation for α. The angle 13.9° was chosen as it is one of the two angles for which the distribution function obtained from (19) coincides exactly with the assumed form of the Onsager trial function, (1), in the nematic phase. The angle 37.8° was chosen because the ratios of the distribution functions in the nematic phase given by (1) and (19) are equal at 0 and 37.8°.

As a test of the sensitivity of the results to these choices, we varied the matching angles for the case $\theta_n = 90°$. Changing the angle used in eq 29 to the second value 33.8° for which the nematic-phase predictions of (19) and (1) coincide leads to a 1.4% decrease in the predicted value of the surface tension. Using 13.9 and 33.8° in place of 0 and 37.8° in (30) increases the computed surface tension by 2.2%.

Equations 29 and 30 give rise to $4H_\infty/\Delta z$ nonlinear integral equations for n and α at the grid points. These equations were solved by a pseudo-temporal iteration scheme formulated by adding a term dn/dt to the left-hand side of (29) and a term $d\alpha/dt$ to the left-hand side of (30). At each iteration, the plane $z_1 = 0$ was adjusted to enforce (11). This required shifting the grid points; the values of n and α at the new grid points were determined by linear interpolation between the previous grid points and the values of n and α were taken to be equal to their bulk values for $|z_1| > H_\infty$. The progress of the iteration was monitored using the interfacial width ζ defined in (13). For sufficiently small time steps, the iteration converged exponentially. The computation was considered complete when ζ was converging exponentially and was within 0.1% of its asymptotic value.

In addition to computing the interfacial structure using the standard axisymmetric Onsager trial function over a range of values of θ_n, we will explore the effects of the nonaxisymmetry of the distribution function for the case $\theta_n = 90°$. To model nonaxisymmetric distributions we adopt the following biaxial generalization of Onsager's trial function

$$f = k \cosh\left(\left[1 - \frac{\sin^2\theta(\cos^2\phi + \beta^2 \sin^2\phi)}{\max(\beta^2, 1)}\right]^{1/2} \alpha\right) \quad (31)$$

where θ is the angle between the rod's axis and the director (x axis) and ϕ is the angle between the projection of the rod axis into the zy plane and the normal to the interface (z axis). The two parameters α and β characterize the orientation distribution and k is a normalization constant that must be determined by numerical integration of (2). This biaxial distribution reduces to Onsager's axisymmetric trial function when $\beta = 1$.

When using the nonaxisymmetric trial function, we apply eqs 29 and 30 at $\phi = 0$ to determine n and α. An equation for β should characterize the non-axisymmetry

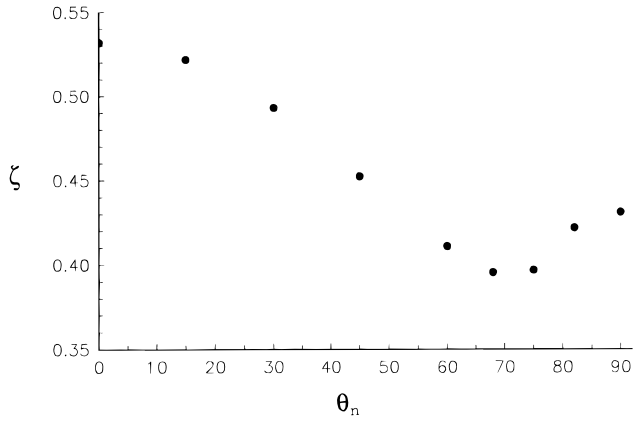

Figure 1. Interfacial thickness non-dimensionalized by rod length, *i.e.*, ζ, plotted as a function of the angle θ_n between the director and the normal to the interface.

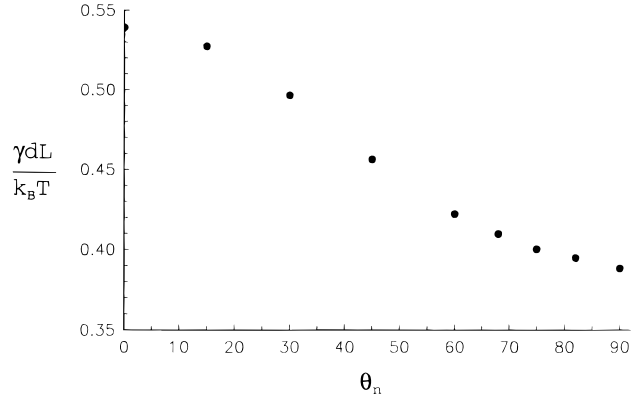

Figure 2. Surface tension nondimensionalized by k_BT/dL plotted as a function of θ_n.

of the distribution and so we require that the ratio of the distribution functions given by (31) and (19) for $\theta = 37.8°$ coincide at $\phi = 0$ and 90°, *i.e.*

$$\frac{P(z_1, \theta_1 = 37.8°, \phi_1 = 0°)}{P(z_1, \theta_1 = 37.8°, \phi_1 = 90°)} = \exp[J(z_1, \theta_1 = 37.8°, \phi_1 = 90°) - J(z_1, \theta_1 = 37.8°, \phi_1 = 0°)] \quad (32)$$

The pseudo-temporal iteration scheme for β is obtained by adding a term $(\alpha + 1)d\beta/dt$ to the left-hand side of (32).

4. Results and Discussion

The interface width ζ and surface tension γ obtained using an axisymmetric trial function are plotted as functions of the angle θ_n between the director and the normal to the interface in Figures 1 and 2, respectively. The width of the interface varies between $0.396L$ and $0.532L$. This confirms that the interface is actually thinner than a rod length and an expansion based on the assumption that the gradients in the rods' probability density are small over a rod length is inappropriate. The interfacial width calculated here is about a factor of two smaller than that obtained using a small gradient expansion by Doi and Kuzuu.[8] For example, we obtain $\zeta = 0.431$ at $\theta_n = 90°$, while Doi and Kuzuu obtained $\zeta = 0.884$.

The surface tension non-dimensionalized by $k_BT/(dL)$ (Figure 2) decreases monotonically with increasing θ_n

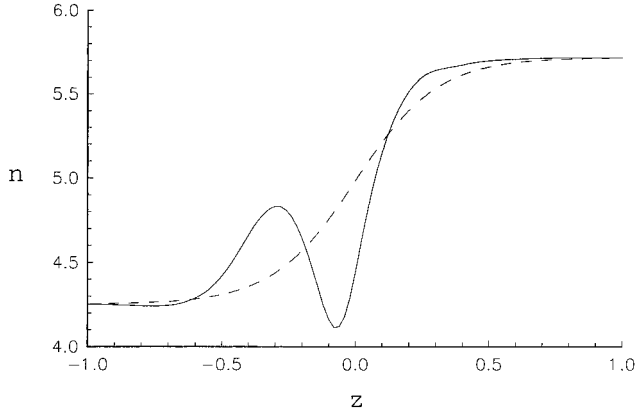

Figure 3. Spatial variation of rod number density across the interface with the director tangent to the interface. The solid line is the computed profile. The dashed line is Doi and Kuzuu's trial function, (6), with the value of δ chosen to produce the computed interfacial width.

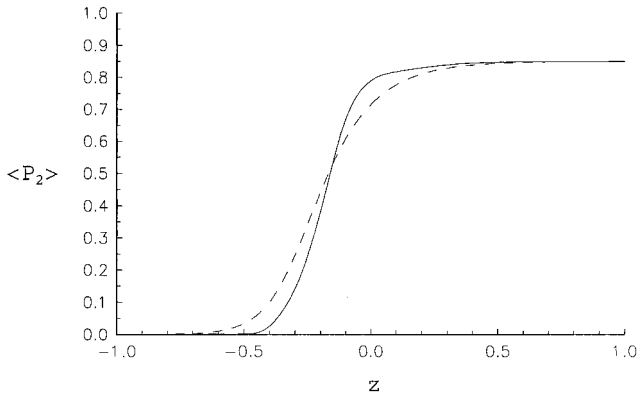

Figure 4. Spatial variation of the order parameter with the director tangent to the interface. The solid line is the computed profile and the dashed line is Doi and Kuzuu's trial function, (5).

from a value of 0.539 at $\theta_n = 0°$ to 0.388 at $\theta_n = 90°$. This indicates that the minimum free energy per unit area of interface occurs for a director that is tangent to the interface. Thus, it is this configuration that will be observed in practice whenever there is sufficient volume in the drop for the director to rotate into a tangent alignment. Doi and Kuzuu also obtained a monotonic decrease in γ with increasing θ_n and in fact their estimates of the surface tension (0.426 at $\theta_n = 0°$ and 0.257 at $\theta_n = 90°$) are surprisingly close to the values computed here.

The spatial variation of the number density n and order parameter $\langle P_2 \rangle$ (defined in (3)) are plotted as the solid lines in Figures 3 and 4, respectively, for a tangent director, $\theta_n = 90°$. While the order parameter grows monotonically from 0 in the isotropic phase to its value, 0.847, in the nematic phase, the rod concentration exhibits a nonmonotonic behavior. Starting from the isotropic phase value of 4.25, the number density first grows and passes through a maximum of 4.83 and then decreases to a minimum $n = 4.11$ that is *smaller* than the concentration in the isotropic phase before growing again to each the nematic phase value, $n = 5.71$. The maximum in the number density occurs at a distance of approximately $0.5L$ from the point $z = 0.1L$ where the order parameter approaches its bulk nematic phase value. The peak and trough in the number density can be rationalized by thinking of the high-concentration, bulk nematic phase ($z > 0.1L$) as a wall excluding the

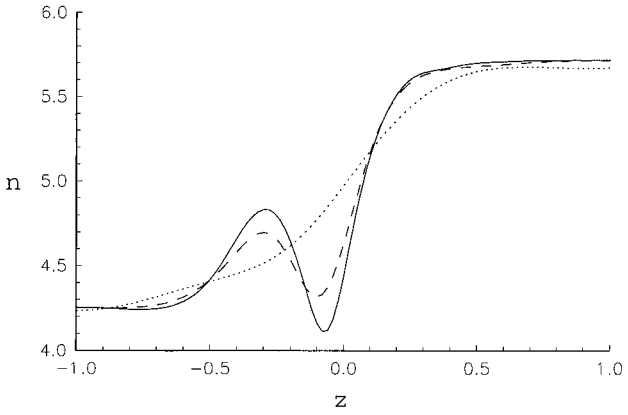

Figure 5. Spatial variation of rod number density for $\theta_n = 90°$ (solid line), $\theta_n = 68°$ (dashed line), and $\theta_n = 0°$ (dotted line).

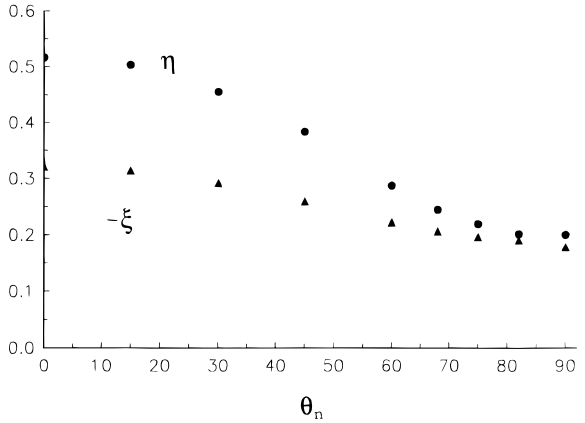

Figure 6. Width, η (circles), and position of the midplane, ξ (triangles), of the interface plotted as functions of the angle between the director and the interfacial normal. Cf. (35) and (33).

fibers in the isotropic phase and interfacial region. The excluded volume is large for fibers whose centers are within half a fiber length of this "wall" and whose axes are not nearly aligned with the director and so there is a deficit of rods in this region.

For comparison with the computed number density and order parameter profiles (solid lines), we have shown the shape of the spatial profiles (5,6) assumed by Doi and Kuzuu as dashed lines in Figures 3 and 4. The value of δ in (5,6) has been chosen to match the interfacial width ζ of the computed profile. The number density profile assumed by Doi and Kuzuu does not include the maximum and minimum in number density observed in our calculation. Indeed, Grosberg and Pachomov[9] have noted previously that Kuzuu and Doi's trial function exhibits only one of several possible shapes for the spatial profile of polymer concentration at a liquid crystalline polymer interface. Doi and Kuzuu's trial function for the order parameter comes closer to capturing the actual shape of the order parameter variation. However, the computed order parameter variation is steeper and shifted to the right.

Figure 5 illustrates the variation of the shape of the number density profile with director angle. The solid line corresponds to a tangent director, the dashed curve to $\theta_n = 68°$, and the dotted line to a perpendicular director, $\theta_n = 0°$. It may be seen that the amplitude of the intermediate peak and valley of rod concentration decreases with decreasing θ_n and eventually disappears. In addition, the interface becomes broader as $\theta_n \rightarrow 0°$. It may be noted from Figure 1 that the interface thickness ζ defined in terms of the number density by (13) decreases as θ goes from 0 to 68° but then passes through a minimum and grows slightly as one approaches tangent alignment $\theta_n = 90°$. This increase in ζ may be attributed to the formation of the intermediate peak in the number density profile. If we compare the dashed and solid lines in Figure 5, it may be seen that the maximum slope in number density continues to increase with increasing θ_n even in the range $68° < \theta_n < 90°$.

Alternative measures of the mean position of the interface, ξ, and the interfacial width, η, defined in terms of the spatial variation in the order parameter, are

$$\int_{-\infty}^{\infty} dz_1 \, [\langle P_2 \rangle - \langle P_2 \rangle_N H(z - \xi)] = 0 \qquad (33)$$

where $H(z)$ is the unit step function

$$H(z) = \begin{cases} 0 & z < 0 \\ 1 & z > 0 \end{cases} \qquad (34)$$

and

$$\eta = \frac{2}{\langle P_2 \rangle_N} \int_{-\infty}^{\infty} dz_1 \, |\langle P_2 \rangle - \langle P_2 \rangle_N H(z - \xi)| \qquad (35)$$

Here $\langle P_2 \rangle_N = 0.847$ is the value of the order parameter in the nematic phase. The width η and shift $-\xi$ of the order parameter variation are plotted as a function of θ_n in Figure 6. It may be seen that η shows a monotonic variation with respect to θ_n. This observation is consistent with our interpretation of the minimum in ζ as arising from the nonmonotonic nature of the number density profie.

The orientation distribution in a bulk nematic liquid crystal is axisymmetric. However, when the director is tangent to the interface (the preferred orientation), the presence of the interface will break the axisymmetry. If we define Cartesian coordinates, with the *x*-axis parallel to the director and the *z* axis normal to the surface, the orientation distribution in *xz* plane is expected to differ from that in the *yz* plane. In particular, one might expect the rods' orientation in the *z* direction to decrease more rapidly than their orientation in the *y* direction. To model nonaxisymmetric distributions, we use the biaxial trial function, (31).

Since this more general distribution function removes the constraint of axisymmetry from the rod distribution function, it will allow the interfacial region to achieve a lower free energy. Consequently, the surface tension obtained for the preferred orientation $\theta_n = 90°$ with the non-axisymmetric distribution is $\gamma = 0.316$, which is 19% smaller than the value obtained with the axisymmetric trial function. The interfacial width $\zeta = 0.394$ defined in terms of *n* is slightly smaller than that ($\zeta = 0.431$) obtain for the axisymmetric trial function, while the width defined in terms of the order parameter variation is larger ($\eta = 0.242$) for the biaxial than ($\eta = 0.200$) for the axisymmetric trial function.

Figure 7 illustrates the spatial variation of the order parameter $\langle P_{2i} \rangle$ measured relative to the *i* axis for *i* =

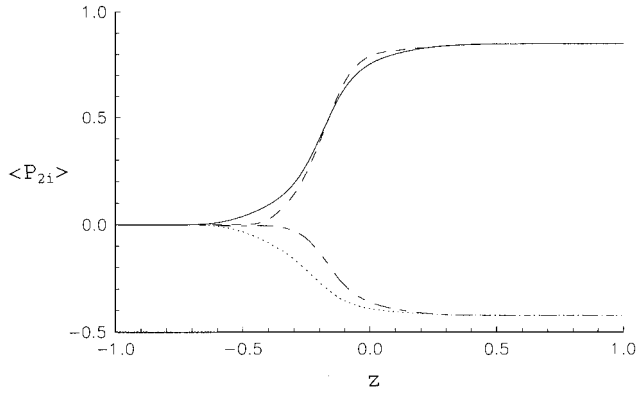

Figure 7. Order parameters defined by (36) obtained using a nonaxisymmetric trial function plotted as a function of position. The director is tangent to the interface. The solid line is $\langle P_{2x}\rangle$, the short-long dashed line $\langle P_{2y}\rangle$, and the dotted line $\langle P_{2z}\rangle$. For comparison, the order parameter $\langle P_{2x}\rangle$ obtained with an axisymmetric trial function is shown as the dashed line.

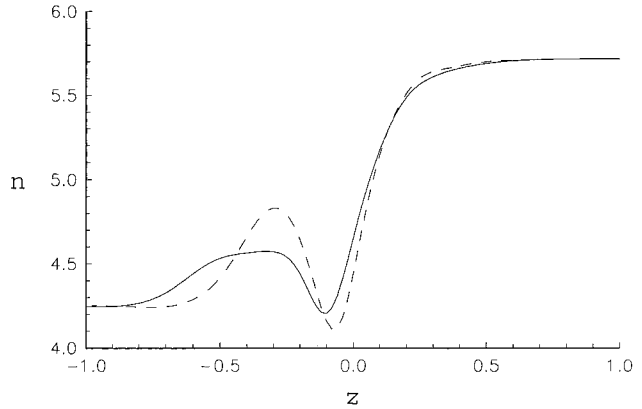

Figure 8. The rod number density profile for the nonaxisymmetric trial function (solid line) is compared with that for the axisymmetric trial function (dashed line). The director is tangent to the interface.

x, y, z. Here

$$\langle P_{2i}\rangle = \frac{3}{2}\langle p_i^2\rangle - \frac{1}{2} \tag{36}$$

The solid line is the order parameter measured relative to the director (x axis), the long-short dashed line relative to the y axis, and the dotted line relative to the interfacial normal (z axis). The dashed line is the order parameter relative to the director for an axisymmetric trial function. It can be seen that, as one moves from isotropic to nematic phase, the rods move away from the interfacial normal z faster than they move away from the y direction. The differences in the z position at which z and y ordering occur lead to a more gradual variation of $\langle P_{2x}\rangle$ for the biaxial distribution than that obtained using Onsager's trial function. Figure 8 illustrates the variation of the rod concentration with position. The peak in n is lower and broader for the biaxial trial function (solid line) than for the axisymmetric trial function, but is still clearly evident. Again the broader peak may be attributed to the fact that the ordering in the interfacial normal and neutral directions occurs at different spatial positions.

Chen and Noolandi[11] studied the isotropic-nematic interface for a hard rod solution using an axisymmetric Legendre polynomial expansion for the rods' orientation distribution. The coefficients in the expansion were allowed to vary with position in a manner similar to that adopted for the parameters n, α, and β in our study. However, because of the large number of Legendre polynomials required to represent accurately the orientation distribution, Chen and Noolandi used a relatively coarse spatial grid corresponding to one fourth of a fiber length. They reported a monotonic number density profile and a surface tension of $\gamma = 0.183k_BT/(dL)$. Chen[12] extended the work of Chen and Noolandi by considering a full spherical harmonic expansion for the orientation distribution and computed a slightly smaller surface tension $\gamma = 0.181k_BT/(dL)$.

Table 1. Surface Tension Non-dimensionalized by $k_BT/(dL)$ is Given for Various Trial Functions and Degrees of Spatial Resolution

spatial resolution	trial function	axisymmetric	nonaxisymmetric
coarse	spherical harmonics	0.183	0.181
refined	Onsager	0.388	0.316
coarse	Onsager	0.308	0.270
coarse	adjusted Onsager	0.256	0.253
refined	adjusted Onsager	0.286	0.241

These results differ significantly from those obtained in the present paper where we obtained a nonmonotonic number density profile, observed a significant effect of nonaxisymmetry on the surface tension, and computed significantly higher values for the surface tension. To understand the origin of these discrepancies, we undertook additional calculations which are summarized in Table 1. The first two lines of Table 1 correspond to Chen's results and the results of our calculations described above. To understand the effects of spatial resolution we changed Δz from 0.02 (line 2) to 0.25 (line 3). The coarser mesh yielded a lower surface tension and a smaller difference between the surface tension for the axisymmetric and nonaxisymmetric trial functions. Thus, it appears that poor spatial resolution accounts in part for the low surface tension and small effect of nonaxisymmetry observed by Chen. The coarser mesh also decreased the amplitude of the peak in the number density obtained in our computations from $0.74/(L^2d)$ to $0.10/(L^2d)$ for the axisymmetric trial function and from $0.37/(L^2d)$ to $0.07/(L^2d)$ for the nonaxisymmetric trial function.

Even with a coarse spatial grid, the computed surface tension using the Onsager trial function is higher than that obtained using a Legendre polynomial expansion. One reason for this is simply the differences in the solutions for the bulk phase obtained with Legendre polynomials[5] and the Onsager trial function.[4] The larger concentration difference between the phases predicted by the Onsager trial function leads to a larger difference in the free energy and a higher surface tension. To adjust for this effect, we performed calculations using the Onsager-like trial functions discussed above but applying the integral equation, (19), at $\theta = 13.95°$ and $\theta = 43.26°$ instead of the angles specified in section 3. This choice of angles forces our calculation to reproduce the number density and order parameter for the bulk nematic phase obtained by Lekkerkerker[5] using a Legendre polynomial expansion. With this adjustment (fourth line of the table), the effect of nonaxisymmetry on the surface tension is found to be as small as that obtained by Chen. The remaining difference between the surface tension 0.253 and that obtained by Chen, 0.181, may be attributed to the more accurate representation of the orientation distribution in Chen's calculation. For completeness we have also presented a result for a

spatially resolved calculation with the adjusted Onsager trial function in the final line of the table.

5. Conclusions

In this paper, we have used a generalization of Onsager's approach to determine the spatial-orientational probability density that minimizes the free energy in a spatially varying hard rod solution. This approach was applied to determine the excess surface free energy (or surface tension) of the boundary between isotropic and nematic phases. The excess free energy is smallest for a director that is tangent to the interface indicating that this configuration is the one likely to be encountered in practice. The surface tension was found to be $0.316k_BT(dL)$. The biaxial nature of the rods' orientation distribution has a significant effect on the interface. The rods orient more rapidly away from the interfacial normal than from the neutral direction as one approaches the nematic phase. The surface tension obtained using a biaxial trial function is 19% smaller than that obtained when the orientation distribution is constrained to be axisymmetric. The rod concentration profile across the interface is nonmonotonic; it passes through a maximum and minimum as one progresses from isotropic to nematic phase.

Doi and Kuzuu[8] have analyzed this problem previously using an axisymmetric trial function, an assumed (monotonic) form for the spatial variations of n and $\langle P_2 \rangle$, and a gradient expansion that would only be expected to apply to very diffuse interfaces $\zeta \gg L$. While the current study draws these assumptions into question, Doi and Kuzuu's final result for the surface tension $\gamma = 0.257k_BT/(dL)$ is surprisingly close to that calculated here. Noolandi and Chen[11,12] used a spherical harmonic expansion to represent the rods' orientation distribution and adopted a nonlocal description of the spatial variations. While they provide a more accurate description of the angular dependence of the probability density than that invoked here, Noolandi and Chen used a coarse grid corresponding to a quarter of a rod length. Their failure to observe non-monotonic number density profiles and a significant effect of nonaxisymmetry on the surface tension may be attributed to this poor spatial resolution. Chen[12] obtained a lower surface tension $\gamma = 0.181k_BT/(dL)$ than that computed here. It is likely that the exact value that could be determined with full resolution of both the translational and orientational spaces would be intermediate between the values 0.181 and 0.316. Chen *et al.*[10] have measured the surface tension of the isotropic−nematic interface for a semiflexible polymer (poly(*n*-hexyl isocyanate) in toluene) using a pendant drop technique. This measurement is 1.8 times larger than the value obtained here. However, the flexibility of the polymer implies that a quantitative comparison cannot be expected. The experimental study does confirm the prediction of[8] and the present study that the director will align tangent to the interface.

Acknowledgment. Financial support was provided by the donors of the Petroleum Research Fund, administered by the American Chemical Society.

References and Notes

(1) Baek, S.-G.; Magda, J. J.; Larson, R. G. *J. Rheol.* **1993**, *37*, 1201.
(2) Burghardt, W. R. *Macromolecular Chem. Phys.* **1998**, *199*, 471.
(3) Fraden, S.; Maret, G.; Caspar, D. L. D.; Meyer, R. B. *Phys. Rev. Lett.* **1989**, *63*, 2068.
(4) Onsager, L. *Ann. N.Y. Acad. Sci.* **1949**, *51*, 627.
(5) Lekkerkerker, H. N. W.; Coulon, P.; van der Haagen, R.; Deblieck, R. *J. Chem. Phys.* **1984**, *80*, 3427.
(6) Frank, J. L. *Trans. Soc. Rheol.* **1961**, *5*, 23.
(7) Straley, J. P. *Phys. Rev. A.* **1973**, *8*, 2181.
(8) Doi, M.; Kuzuu, N. *J. Appl. Polym. Sci., Appl. Polym. Symp.* **1985**, *41*, 65.
(9) Grosberg, A. Y.; Pachomov, D. V. *Liq. Cryst.* **1991**, *10*, 539.
(10) Chen, W.; Sato, T.; Teramoto, A. *Macromolecules* **1996**, *29*, 4283.
(11) Chen, Z. Y.; Noolandi, J. *Phys. Rev. A* **1992**, *45*, 2389.
(12) Chen, Z. Y. *Phys. Rev. E* **1993**, *47*, 3765.
(13) Bolhuis, P.; Frenkel, D. *J. Chem. Phys.* **1997**, *106*, 666.

MA980779L